THE ASTROPHYSICAL JOURNAL, 501:386–396, 1998 July 1


# NETWORK CORONAL BRIGHT POINTS: CORONAL HEATING CONCENTRATIONS FOUND IN THE SOLAR MAGNETIC NETWORK

D. A. FALCONER
National Research Council/Marshall Space Flight Center, Space Science Laboratory, Code ES82, Huntsville, AL 35812
AND
R. L. MOORE, J. G. PORTER, AND D. H. HATHAWAY
NASA Marshall Space Flight Center, Space Science Laboratory, Code ES82, Huntsville, AL 35812
*Received 1997 October 3; accepted 1998 February 2*

## ABSTRACT

We examine the magnetic origins of coronal heating in quiet regions by combining *SOHO*/EIT Fe XII coronal images and Kitt Peak magnetograms. Spatial filtering of the coronal images shows a network of enhanced structures on the scale of the magnetic network in quiet regions. Superposition of the filtered coronal images on maps of the magnetic network extracted from the magnetograms shows that the coronal network does indeed trace and stem from the magnetic network. Network coronal bright points, the brightest features in the network lanes, are found to have a highly significant coincidence with polarity dividing lines (neutral lines) in the network and are often at the feet of enhanced coronal structures that stem from the network and reach out over the cell interiors. These results indicate that, similar to the close linkage of neutral-line core fields with coronal heating in active regions (shown in previous work), low-lying core fields encasing neutral lines in the magnetic network often drive noticeable coronal heating both within themselves (the network coronal bright points) and on more extended field lines rooted around them. This behavior favors the possibility that active core fields in the network are the main drivers of the heating of the bulk of the quiet corona, on scales much larger than the network lanes and cells.

*Subject headings:* Sun: corona — Sun: magnetic fields — Sun: UV radiation

## 1. INTRODUCTION

The Sun keeps its outer atmosphere, the corona, heated to million degree temperatures. Because it is so hot, the corona glows in X-rays and extends to great heights, continually expanding and escaping from the Sun to become the super-Alfvénic solar wind that forms the heliosphere, reaching far beyond the planets. While it has been established for decades that the corona and solar wind owe their existence to coronal heating, the heating process remains unknown other than in broad outline. Determination of the specifics of the heating, the main drivers and mechanisms, is a major quest of solar astrophysics.

It is known that most if not all coronal heating is magnetic in origin, an aspect of the Sun's magnetic activity (e.g., Vaiana & Rosner 1978). X-ray and EUV coronal images (such as from *Skylab*, or now from *Yohkoh* and *SOHO*) together with magnetograms plainly show that on the overall scale of active regions and larger ($> \sim 10^5$ km), coronal heating is generally stronger where the magnetic field is stronger, the strongest heating occurring in active regions, which are sites of the strongest magnetic fields found on the Sun. However, within active regions it is often seen that different areas of the same field strength differ greatly in strength of coronal heating (e.g., Falconer et al. 1997). Thus, it is clear that the strong coronal heating in active regions is a result of the strong (greater than $\sim 100$ G) magnetic field but depends on more than the field strength alone.

Falconer et al. (1997) studied the magnetic origins of coronal heating in active regions by registering *Yohkoh* coronal X-ray images with MSFC vector magnetograms and examining the magnetic roots of persistently bright coronal features. In their sample of $\sim 100$ bright coronal features, they found nearly all were rooted near (within $10^4$ km) a neutral line in the photosphere. These bright coronal features were of two basic types: core features and extended loops. A core feature resides within a core magnetic field, a field closely enveloping a neutral line. An extended loop is rooted, at one end, in or around the core field of a neutral line but extends well away from this neutral line and core field. Falconer et al. 1997) found that each bright coronal feature rooted near a neutral line either was one of these two types or was a combination of these two elements. In a large majority of cases (80%), the core field that was near the foot of an extended loop and/or held a core feature was strongly sheared. Furthermore, substructure within the core features continually changed in brightness and form, in the manner of microflaring, on timescales of a few minutes. whereas the extended loops evolved more gradually. From these results, Falconer et al. (1997) concluded (1) that the source of much of the strong coronal heating in active regions, both in the core features and in the extended loops, is the core field low along the neutral lines, (2) that this heating is driven by microflaring activity in the core field, and (3) that the microflaring and coronal heating are more probable and usually stronger when the core field is more strongly sheared and hence holds a larger store of free magnetic energy that might be released to drive the coronal heating. The outstanding result motivating the present paper is that the proximity of a polarity dividing line is a necessary condition for much of the strong coronal heating in active regions.

In this paper, we present evidence suggesting that the close linkage of strong coronal heating with neutral-line core fields in active regions may carry over to the coronal heating in quiet regions. That is, from our observations, we

infer that active core fields on neutral lines in the magnetic network may be the drivers of much of the coronal heating in quiet regions, both in the low-lying magnetic loops within the network (the core fields) and in larger coronal loops and funnels stemming from the network.

Prior to our new, more direct evidence for coronal heating by network core fields, there was a line of previous circumstantial evidence, from observations of quiet regions, that network core fields might be important sources of coronal heating. First, in coronal images of quiet regions covering hundreds of supergranules, such as in Figure 1, there are usually a few outstanding bright compact coronal features (conventionally called coronal bright points), typically 10,000–20,000 km in diameter, somewhat smaller than a supergranule (network cell) but larger than the typical 5000–10,000 km width of the lanes of the magnetic network (Koutchmy 1977; Martres & Bruzek 1977; Dowdy, Rabin, & Moore 1986). These concentrations of coronal heating are seated in similarly compact bipolar magnetic fields and undergo frequent microflaring in coronal and transition-region emission (Koutchmy 1977; Nolte, Solodyna, & Gerassimenko 1979; Habbal & Withbroe 1981). Second, there is an abundance of mixed-polarity magnetic flux in the magnetic network; that is, the network lanes are riddled with neutral lines (Dowdy et al. 1986). Third, Porter et al. (1987) found frequent microflaring in transition region

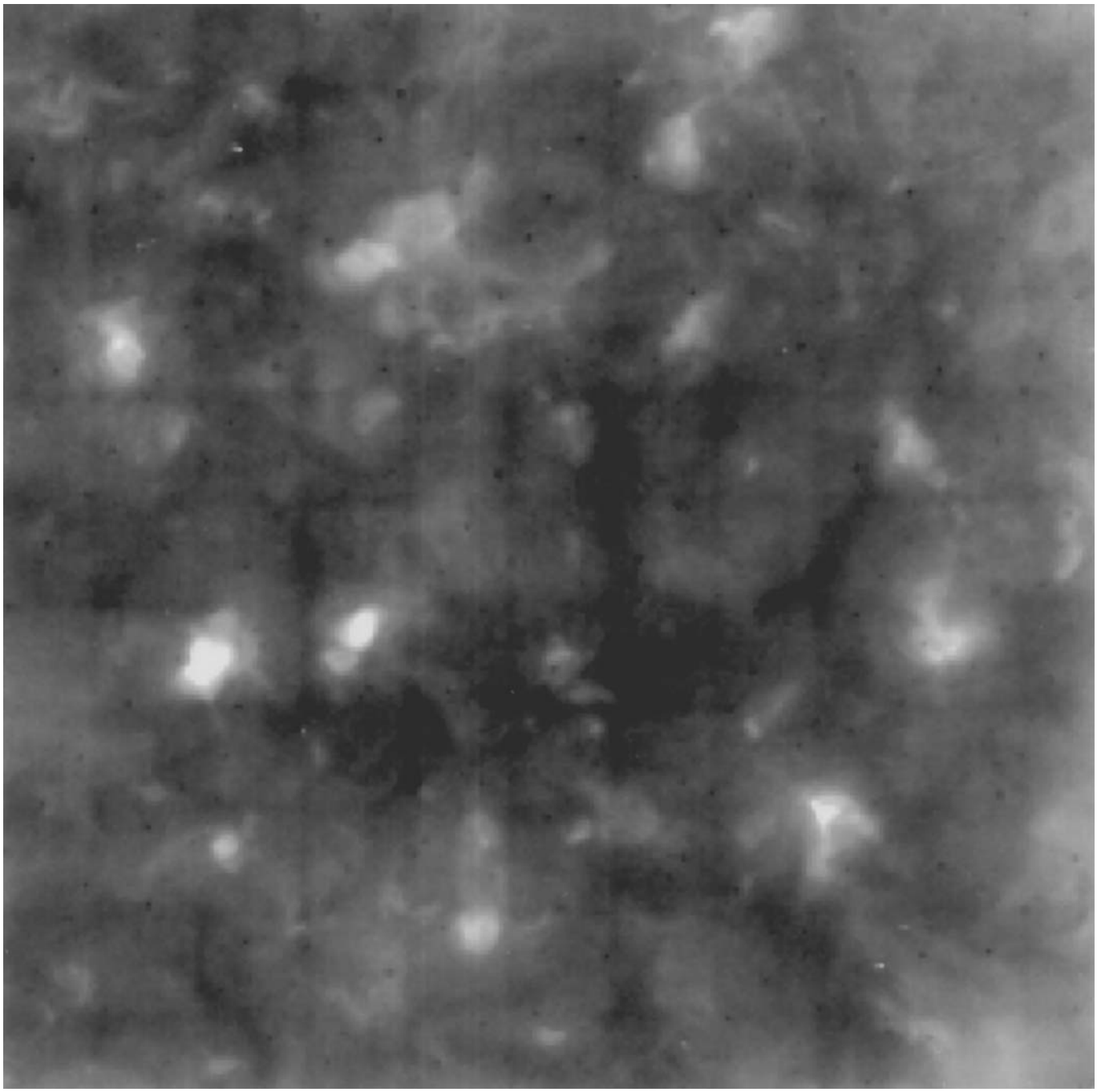

FIG. 1.—Fe XII quiet corona. This image is part of a full-disk Fe XII 195 Å image from *SOHO*/EIT on 1996 March 16. The field of view here is 0.6 $R_\odot$ square, centered on the disk. There are both compact bright features and larger, more diffuse bright regions. The larger compact bright features are conventional coronal bright points. Smaller bright points are also seen down to the limit of resolution (1 pixel). North is up and east is to the right.

($T \sim 10^5$ K) emission at many neutral lines in the magnetic network. Thus, there was reason to expect that microflaring in some of the neutral-line core fields in the magnetic network might heat enough plasma to coronal temperatures to be visible in coronal images as small coronal bright points, small counterparts to the coronal core features in active regions and to the conventional coronal bright points in quiet regions.

In the Fe XII ($T \sim 1.6 \times 10^6$ K) coronal image in Figure 1, in addition to the few obvious conventional coronal bright points, many further bright points can be seen that are smaller in diameter than the typical width of magnetic network lanes (<10,000 km). Are these small coronal bright points our expected network coronal bright points? We address this question by examining the location of Fe XII small coronal bright points relative to the magnetic network lanes and relative to neutral lines within the lanes. From a sample of a few hundred small coronal bright points observed in quiet regions like that in Figure 1, we find that a large majority lie within or touch the network magnetic flux and that there is a very significant incidence of small coronal bright points on neutral lines in the network. These results indicate that most small coronal bright points are seated in network core fields, showing that network core fields often have significant local coronal heating within them. This, along with the similarity of the magnetic setting of network core fields to that of core fields at the feet of extended coronal loops in active regions, makes network core fields stronger candidates for driving coronal heating not only within themselves but also on extended magnetic field lines stemming from the network lanes.

## 2. DATA SELECTION AND PREPARATION

The data used in this study are from full-disk coronal images and concurrent full-disk photospheric magnetograms. The coronal images are Fe XII (195 Å) filtergrams from the *Solar and Heliospheric Observatory*'s Extreme-Ultraviolet Imaging Telescope (*SOHO*/EIT) (Delaboudiniere et al. 1995). Of the four EIT filters, the Fe XII filter gives the best sensitivity to plasma at quiet coronal temperatures ($T \sim 1$–$2 \times 10^6$ K) and neglible sensitivity to transition region plasma ($T < 10^6$ K). These images have enough spatial resolution (2.″6 pixels) to resolve features smaller than the width of network lanes. The magnetograms are from the National Solar Observatory/Kitt Peak (Jones et al. 1992). These show the photospheric field well enough for our study, having a spatial resolution of a few arcseconds or better (set by the seeing at Kitt Peak) and a noise level of less than 3 G for 2.″3 pixels. (The original magnetograms have 1.″15 pixels, but the data that we used were summed in 2.″3 pixels. This gives spatial resolution comparable to that of the coronal images and reduces the noise level of the magnetogram.)

For our study we selected six full-disk Fe XII images, each from a different day. The selection criteria were the following: (1) there were no active regions within $\sim 0.5\ R_\odot$ of disk center, (2) there was a good quality Kitt peak magnetogram for that day, and (3) the time of the Fe XII image was within 2.5 hr of the middle of the hour-long Kitt Peak magnetogram scan. On the scales resolved in our data, we expect little change in the magnetic network in less than a few hours (Wang, Zirin, & Ai 1991). The selected coronal images and corresponding magnetograms are listed in Table 1. To limit projection offsets between coronal bright points and the photospheric magnetic flux structure, we limited our study to a central area of the disk, the area covered by a $0.6\ R_\odot$ square field of view centered on the disk. This part of the full-disk coronal image for one of our six days is shown in Figure 1; the matching area of the magnetogram for that day is shown in Figure 2. The six areas together had hundreds of small coronal bright points, enough for obtaining significant statistics on the magnetic location of these coronal heating concentrations.

TABLE 1

OBSERVATIONS

| Date | EIT Fe XII Image (UT) | Kitt Peak Magnetogram (UT) |
|---|---|---|
| 1996 Nov 10..... | 18:20 | 16:58 |
| 1997 Feb 10 ..... | 19:55 | 17:43 |
| 1997 Feb 19 ..... | 19:13 | 18:09 |
| 1997 Mar 4 ..... | 19:29 | 17:58 |
| 1997 Mar 6 ..... | 19:21 | 19:41 |
| 1997 Mar 16..... | 19:13 | 17:48 |

Each coronal image was registered to its magnetogram by registering the solar limbs of the two full-disk images and then shifting the magnetogram to compensate for the solar rotation during the time between the two observations. By this procedure, the coronal image was registered to the magnetogram to well below the size of the network and emission features of interest in our central $0.6\ R_\odot$ square. This accuracy was estimated both from the registration of the conventional coronal bright points with their magnetic bipoles, and, a posteriori, from finding that 1 pixel shifts in the registration begin to decrease the population of small bright points in the magnetic network lanes. A shift of half a network cell completely destroys the strong correlation found with no shift.

The quiet Fe XII corona (Fig. 1) has both a diffuse, large-scale brightness component (haze), and compact bright features, on the size scales of the magnetic network. The scale of the compact features ranges down to 1 pixel (2.″6) in size. To study these small bright features we need to be able to identify them objectively. We designed an algorithm to mimic how the eye selects bright points. The algorithm suppresses the large scale component by first using a square smoothing function about two-thirds of a network cell wide (11 pixels or 21,000 km) with a central square about one-third of a network cell wide (5 pixels or 9000 km) removed (resembling a picture frame; see Fig. 3) to define a "local background" brightness level for each pixel of the coronal image. Then, because the eye recognizes a feature by its relative enhancement and not by an absolute enhancement, we divide the original image by this background image, resulting in a normalized filtered image (Fig. 3). The enhanced emission seen in Figure 3 is only a small fraction (about 5%) of the total Fe XII emission (Table 2). The other 95% of the total emission is the background haze. The presence of this strong background is why we need to filter the *SOHO*/EIT Fe XII images to make the network-scale coronal structures more obvious. We define a bright point as any contiguous set of pixels (including diagonally) in which emission is enhanced by 30% or more above the background because these conditions select those features that strike the eye as bright points in the unfiltered coronal images. This systematically selects both conventional bright points and smaller bright points.

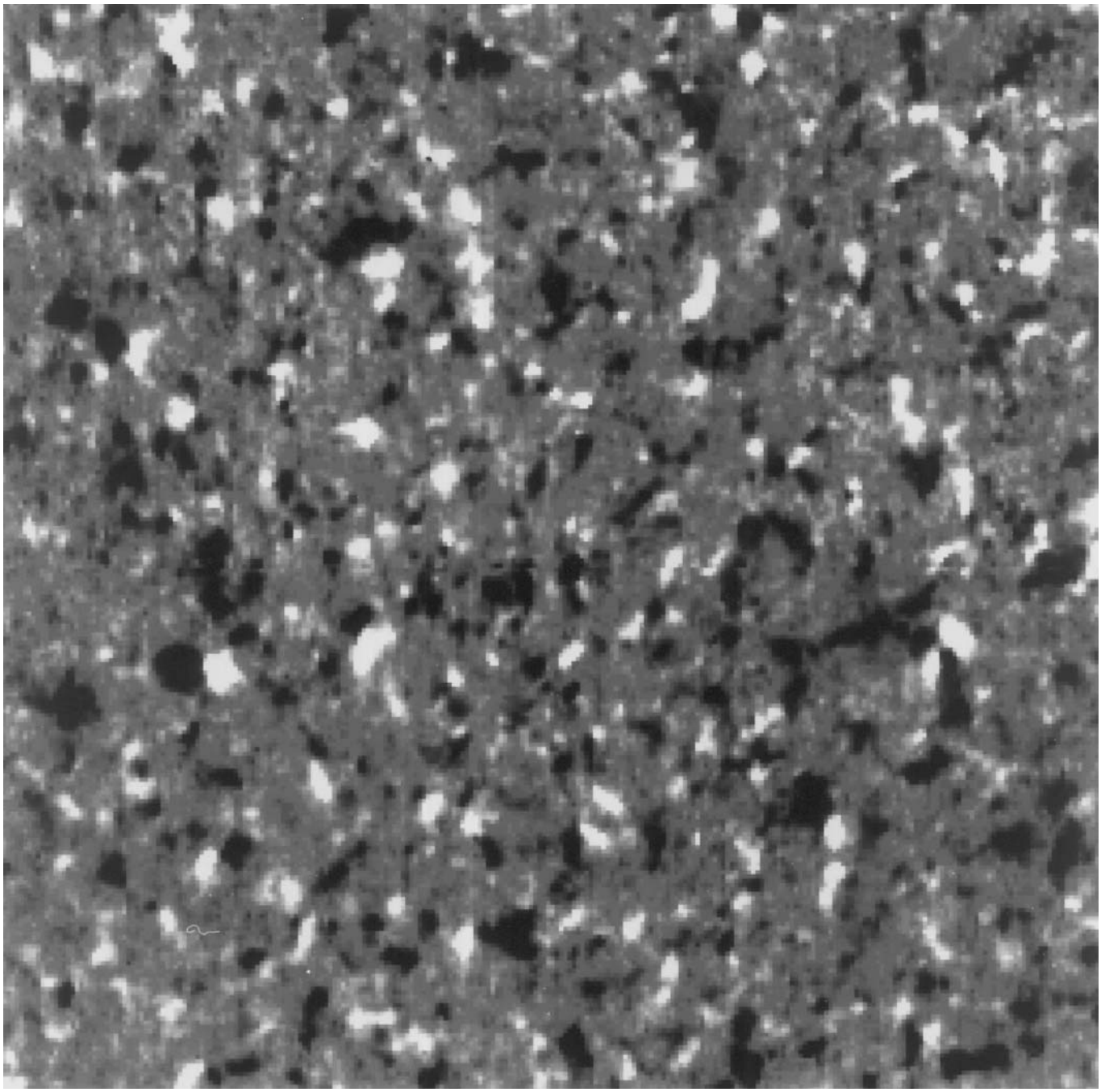

FIG. 2.—Kitt Peak magnetogram of the solar area viewed in Fig. 1. This magnetogram was taken about 1.5 hr before the coronal image.

The magnetic network is extracted from a Kitt Peak magnetogram by a three-step process that brings out the network lanes relative to the cell interiors. First, a $3 \times 3$ pixel boxcar smoothing function is applied to the absolute flux. Second, those pixels with smoothed flux less than 3 G are masked out. The unmasked pixels are mainly those with network magnetic field. Third, we retain only the sign of the unsmoothed magnetic field in the unmasked pixels, leaving the magnetic network map, as in Figure 4, in which each pixel is marked as being below threshold, or having positive field above threshold, or having negative field above threshold. This process filters out the weak fine-scale salt and pepper in the cell interiors, leaving the magnetic network and network neutral lines intact. There is no loss of spatial resolution within the network lanes: all neutral lines in these areas of the unsmoothed magnetogram (with 2.″3 pixels) are retained in the map of the lanes. Approximately 25% of the area is covered by the network lanes in these maps.

## 3. RESULTS

Superposition of the unfiltered coronal images on the magnetic network maps shows, as in Figure 5, that over most interiors of magnetic network cells the corona is slightly dimmer than over the surrounding network lanes. That is, when superposed on the magnetic network, the unfiltered coronal images suggest that there is a faint network of coronal structures rooted in the photospheric magnetic network. This coronal network is verified and clarified in the filtered coronal images (Fig. 3), which

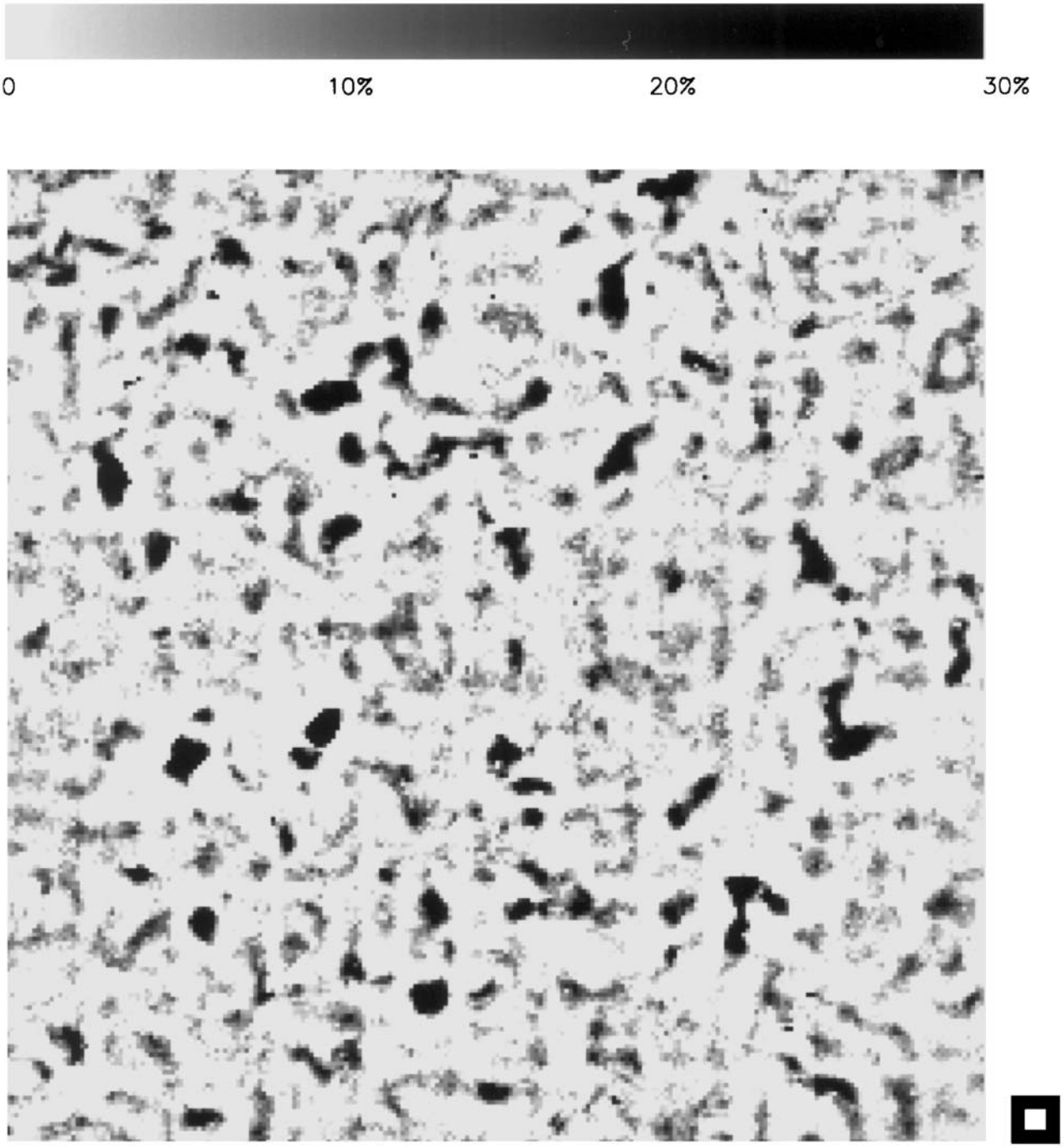


FIG. 3.—Spatially filtered coronal image showing network scale and finer coronal structure extracted from the image in Fig. 1. The large spatial scale features have been filtered out by using a picture frame filter (shown to scale, *lower right*), leaving the small spatial scale enhanced features. The degree of a pixel's enhancement over the local background is shown by its darkness with enhancements of 30% or larger being black. White pixels are those that are no brighter than the local background.

suppress the bright haze of the overlying large scale quiet corona. Superposition of the filtered coronal images on the magnetic network maps, as in Figure 6, confirms that the coronal network stands on the magnetic network. The spatial correspondence of the two networks is quantified in Table 2. Table 2 shows that the brighter components of the coronal network lie more within the magnetic network lanes than do the fainter components. Table 2 also shows that even when the faintest parts (everything above 0%) are included in the coronal network, there is still some overall concentration in the magnetic areas of the magnetic network maps (33% compared to the 25% expected from the area of the magnetic network, if there were no correlation of the coronal network with the magnetic network). In Figure 7, only the coronal bright points (coronal brightness enhancements of more than 30%) from the filtered coronal image are superimposed on the magnetic network map. This shows that nearly all bright points overlie or touch network magnetic flux and that many bright points are on network neutral lines. All of the conventional coronal bright points (diameters $\geq 10^4$ km) in Figure 7 sit on neutral lines in prominent magnetic bipoles; many smaller bright points sit on neutral lines as well.

To estimate the significance of the apparent associations

TABLE 2

PROPERTIES OF THE Fe XII CORONAL NETWORK: AREA COVERAGE, EMISSION CONTRIBUTION, AND CONCENTRATION IN MAGNETIC NETWORK

| Coronal Brightness Enhancement | Area Coverage (%) | Enhanced Emission[a] Contribution (%) | Fraction of Coronal Network in Network Magnetic Area (%) |
|---|---|---|---|
| >30% ..... | 1.9 | 1.5 | 68 |
| >15% ..... | 6.3 | 2.5 | 53 |
| >10% ..... | 11 | 3.2 | 46 |
| >5% ..... | 23 | 4.0 | 39 |
| >0% ..... | 42 | 4.5 | 33 |

[a] Each entry in this column gives, for the total Fe XII coronal emission from our six quiet regions, the fraction contributed by the enhanced emission from the areas having enhanced emission above the level given in the first column. The enhanced emission in a pixel is the total emission in the pixel minus the local background emission in that pixel. Nearly all of the background emission is from the diffuse extended corona, the components of which have scales larger than the width of the network lanes.

noted in Figure 7, we sort the bright points into bins by size and compare the association with magnetic features to that given by random chance. The bright points in each bin are twice the size of those in the preceding bin, with the smallest two bins being 1 pixel, and 2–3 pixels (Table 3). The two largest sizes span conventional coronal bright points, while the others cover the smaller coronal bright points. For each bin we first find the number of bright points overlying or

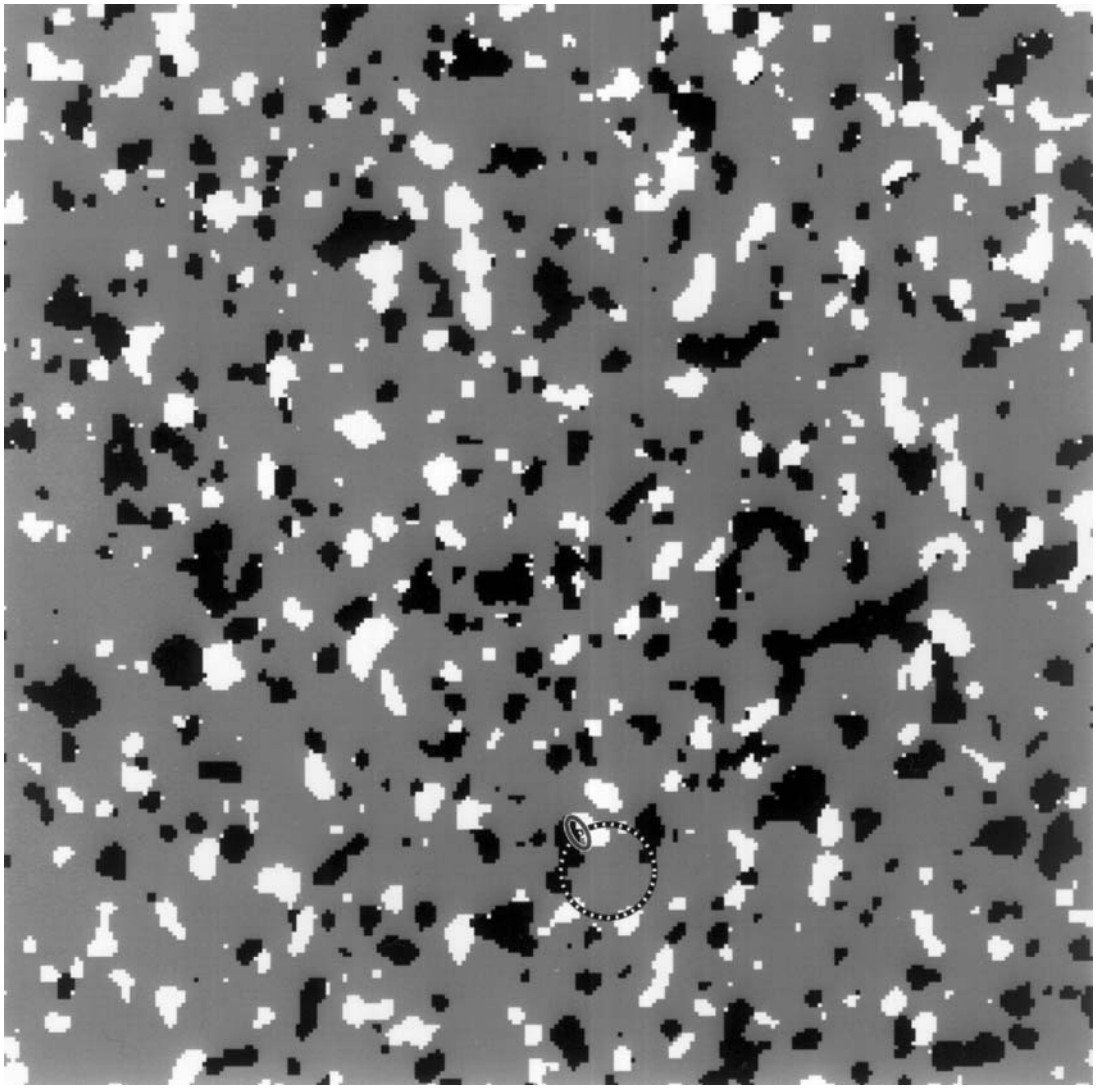

FIG. 4.—Magnetic network map obtained from the Kitt Peak magnetogram in Fig. 2. This map is the result of a filtering/masking procedure that cleans out the cell interiors and leaves network lanes (see text). Areas below threshold in the magnetic flux are gray; areas above threshold (3 G) are white for positive flux and black for negative flux. The black and white circle links the magnetic flux patches of the network lane around a typical network cell. The dark gray oval has roughly the extent of the core field encasing a typical neutral line in the network lane.

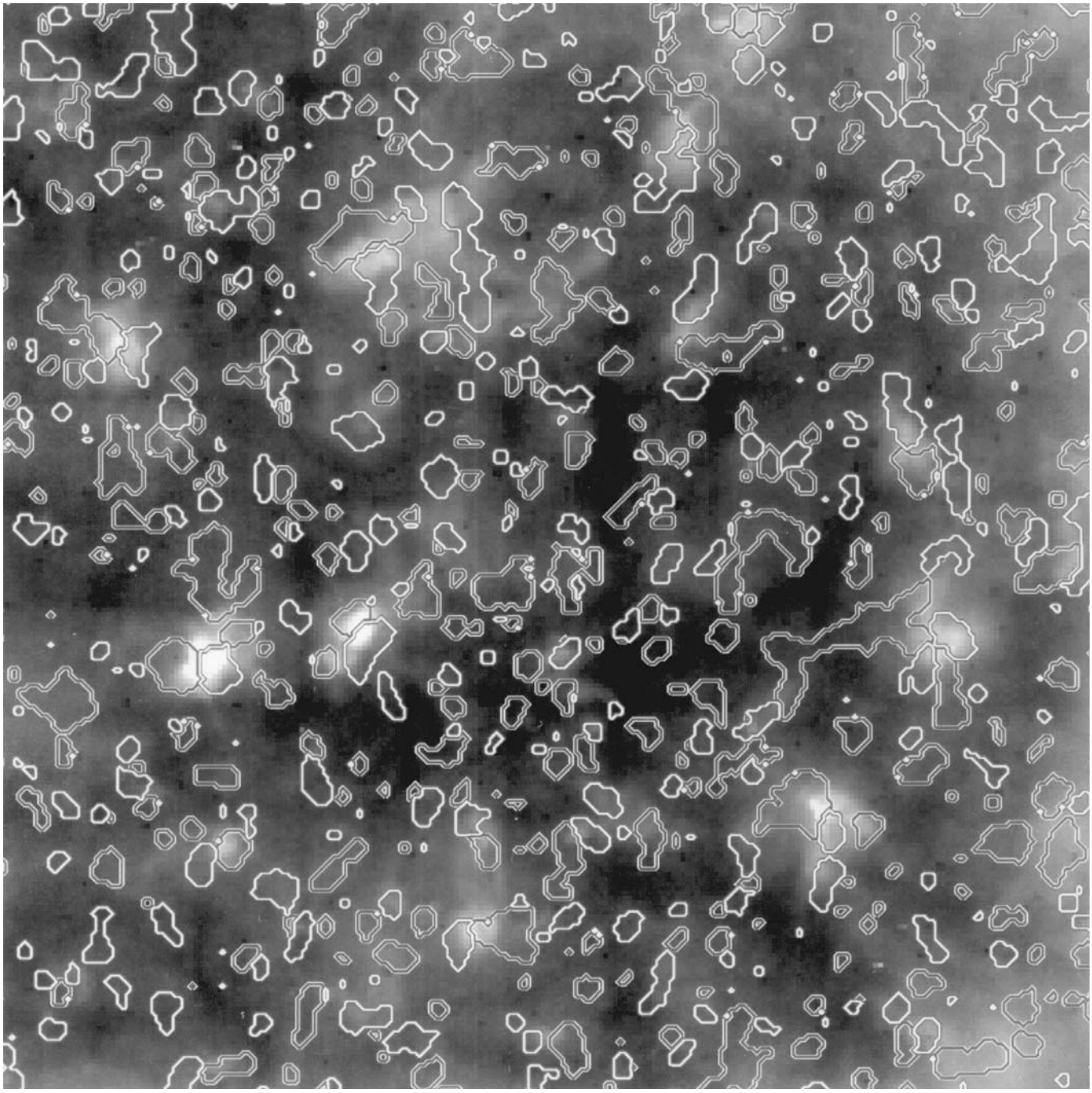

FIG. 5.—Fe XII corona registered with its magnetic network map. The Fe XII image is from Fig. 1; the magnetic network map is from Fig. 4 with positive flux outlined in white and negative flux in gray. The largest bright points coincide with magnetic bipoles as do many of the smaller bright points. The network cell interiors tend to be dimmer than the network lanes.

touching any magnetic area (the network lanes) in the network maps.

Next, we need to assess how many bright points (what fraction) would be expected to hit the network by random chance. For 1-pixel bright points this fraction equals the fracton of the area that overlies or touches magnetic areas of the maps, but for larger bright points the situation is more complicated because the sizes and shapes of the network cells and bright points come into play. It would be possible to estimate the fraction of hits, $\pi$, expected for random chance using a Monte Carlo simulation. However, this would require construction of models for both the network configuration and bright point sizes and shapes. Instead, we chose to estimate the numbers of hits expected from random chance by using the actual observations, rotating and flipping the bright point map into seven different incorrect orientations on the magnetic network map. For network bright points (those smaller than 25 pixels in area), this provides us $7 \times 100$ or so test bright points per bin to estimate the fraction that would hit the magnetic network by random placement (see Table 3). As expected, large bright points have a higher random probability than small bright points of overlying or touching magnetic network because of their size (Table 3).

Now that we know for each bin the number of bright points, $N$; the number of bright points overlying or

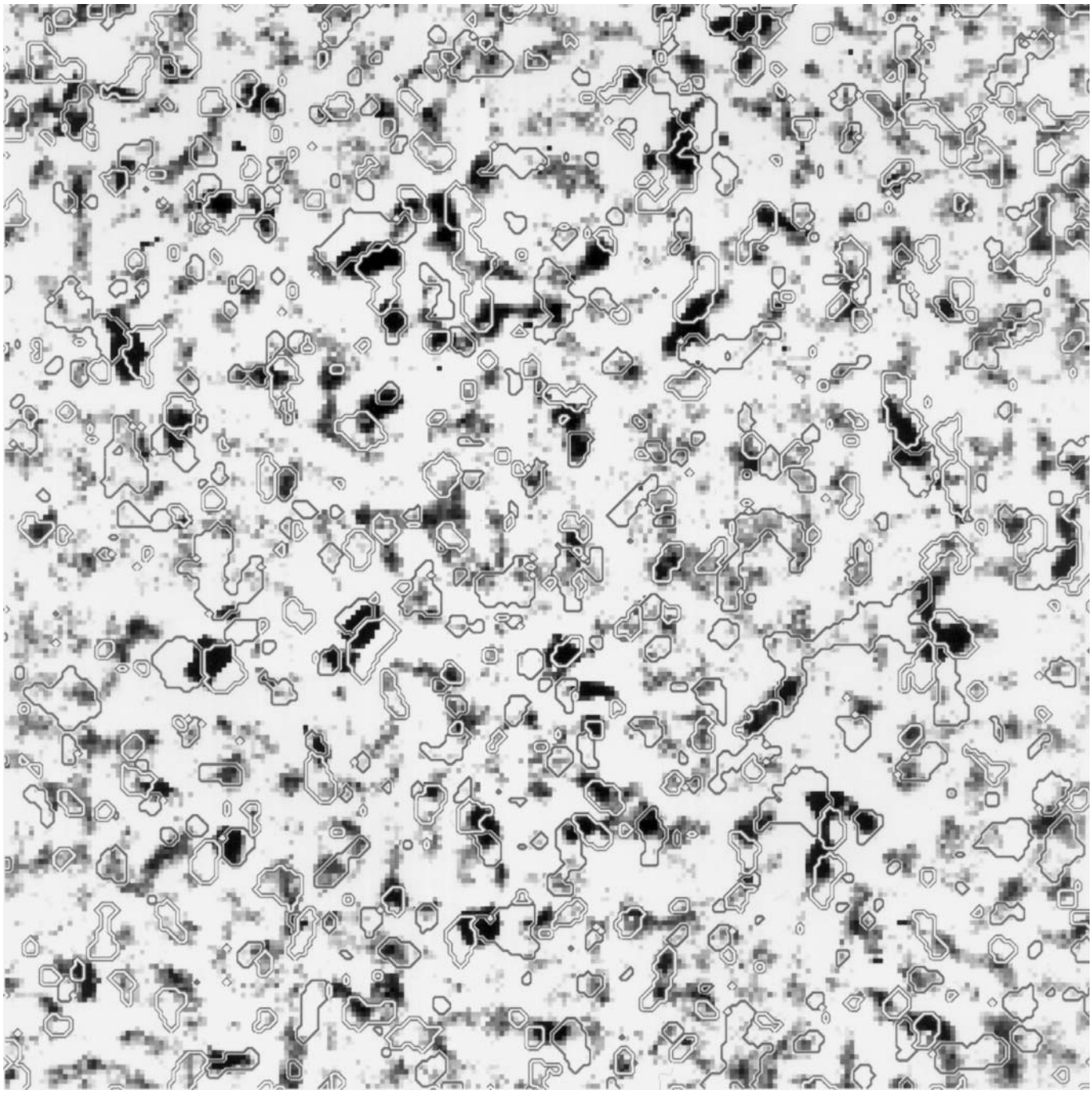

FIG. 6.—Filtered Fe XII image registered with the magnetic network map. The filtered Fe XII image mainly consists of bright points in the magnetic network along with fainter features that either trace the magnetic network or appear to be rooted in the network and arch across cell interiors.

touching the network, $R$; and the fraction that would be expected by random chance, $\pi$, we can use the binomial probability formula to estimate the probability $P$ of getting the result $R$:

$$P(R, N, \pi) = \frac{N!\pi^R(1-\pi)^{(N-R)}}{(N-R)!R!} . \quad (1)$$

The significance of getting $R$ hits out of $N$ tries is given by the probability of getting $R$ or more hits out of $N$ tries:

$$\sum_{i=R}^{N} P(i, N, \pi) . \quad (2)$$

Values of $\sum P$ are given in Table 3. We follow the same procedure to determine the significance of the association of bright points with network neutral lines (hits on both polarities at once).

We find a very significant association of small coronal bright points with both the magnetic network Figure 8 and neutral lines in the magnetic network (Fig. 9). Table 3 and Figure 8 show that in each size of bin of small (less than 25 pixels) bright points, the probability that the observed correlation of bright points and magnetic network occurred by chance is less than about $10^{-6}$. The correlation with neutral lines in the network is even more significant ($\sum P < 10^{-11}$) for small bright points of intermediate size

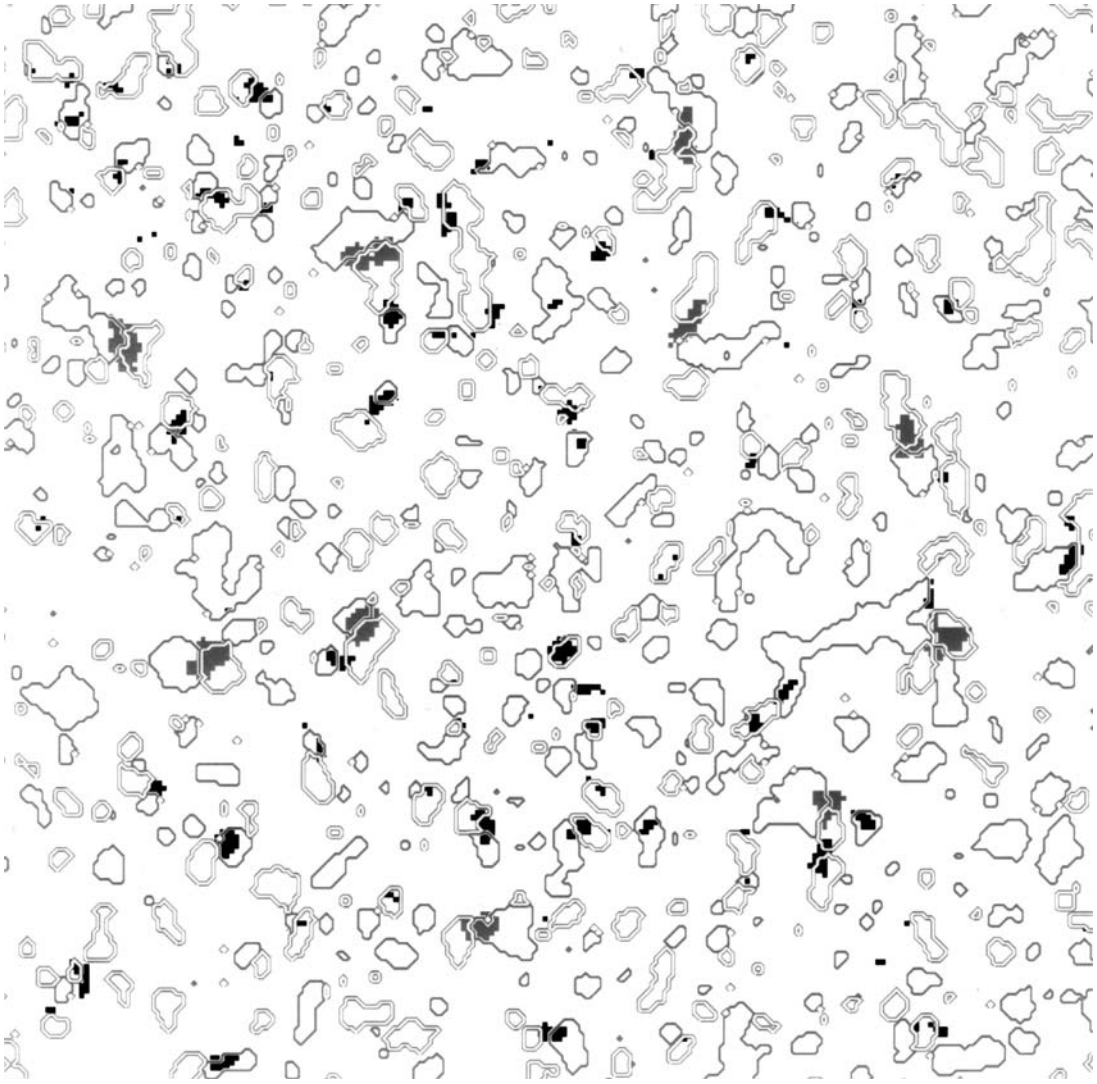

FIG. 7.—Coronal bright points registered with the magnetic network map. This shows that almost all bright points, large and small, are located in or adjacent to the magnetic network, with many on neutral lines. The magnetic network is outlined by the contours: white for positive flux and gray for negative. The conventional bright points ($\geq 25$ pixels in area, or $\geq 10^4$ km in extent) are gray, and the smaller bright points are black. The conventional bright points are all on neutral lines of prominent bipoles. Most of the smaller bright points are on near neutral lines in the network or near the edge of network flux.

(4–24 pixels) (Fig. 9). The significance for larger bright points is less, because of the increased chance of a large bright point to fall randomly on magnetic network. There is a noticeable drop in the significance of 1–3 pixel bright points with neutral lines in the network magnetic field. This is probably because 1–3 pixel bright points can be powered by small unresolved bipoles, or by small bipoles that appeared or disappeared in the time interval between the coronal image and the magnetogram. The fact that the drop

TABLE 3

NONRANDOMNESS OF THE COINCIDENCE OF SMALL CORONAL BRIGHT POINTS WITH NETWORK MAGNETIC FLUX AND NETWORK NEUTRAL LINES

| SIZE BIN (Pixels) | $N$ | TARGET: ANY FLUX | | | | TARGET: BOTH POLARITIES | | | |
|---|---|---|---|---|---|---|---|---|---|
| | | $R$ | $\pi$ | $R/N$ | $\sum P$ | $R$ | $\pi$ | $R/N$ | $\sum P$ |
| 1 ..... | 174 | 145 | 0.58 | 0.83 | $7 \times 10^{-13}$ | 39 | 0.10 | 0.22 | $1 \times 10^{-6}$ |
| 2–3..... | 122 | 105 | 0.63 | 0.87 | $1 \times 10^{-8}$ | 34 | 0.11 | 0.28 | $2 \times 10^{-7}$ |
| 4–6 ..... | 101 | 98 | 0.71 | 0.97 | $1 \times 10^{-11}$ | 49 | 0.18 | 0.49 | $3 \times 10^{-12}$ |
| 7–12 ..... | 99 | 97 | 0.81 | 0.98 | $3 \times 10^{-7}$ | 67 | 0.28 | 0.68 | $3 \times 10^{-16}$ |
| 13–24..... | 94 | 94 | 0.87 | 1.00 | $2 \times 10^{-6}$ | 77 | 0.37 | 0.82 | $5 \times 10^{-19}$ |
| 25–48..... | 48 | 48 | 0.96 | 1.00 | 0.14 | 46 | 0.55 | 0.96 | $3 \times 10^{-10}$ |
| 49+ ..... | 7 | 7 | 0.95 | 1.00 | 0.7 | 7 | 0.67 | 1.00 | 0.06 |

NOTES.—$N$ is the number of bright points; $R$ is the number that hit the target; $\pi$ is the fraction that would hit by random chance; $\sum P$ is the significance of getting $R$ hits out of $N$ shots. For network coronal bright points ($\leq 24$ pixels), the uncertainty in $\pi$ is less than $\pm 0.02$. The uncertainties in $\pi$ produce roughly a factor of 10 uncertainty in the probability.

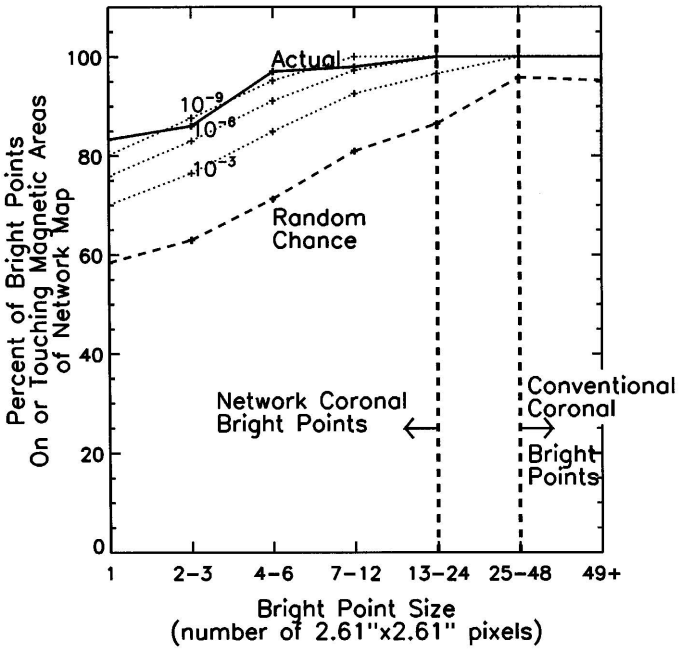


FIG. 8.—Quantification of the strong tendency of small coronal bright points to be located in the magnetic network. This is the result (from Table 3) for all the bright points examined from 6 different days (see text). The fraction of the bright points that touch or overlie magnetic areas of the magnetic network maps is plotted as the solid line; the fraction expected from random chance is the dashed line. Probability levels of $10^{-3}$, $10^{-6}$, and $10^{-9}$ are shown as dotted lines. Only a small fraction of the small bright points do not overlie or touch network magnetic field.

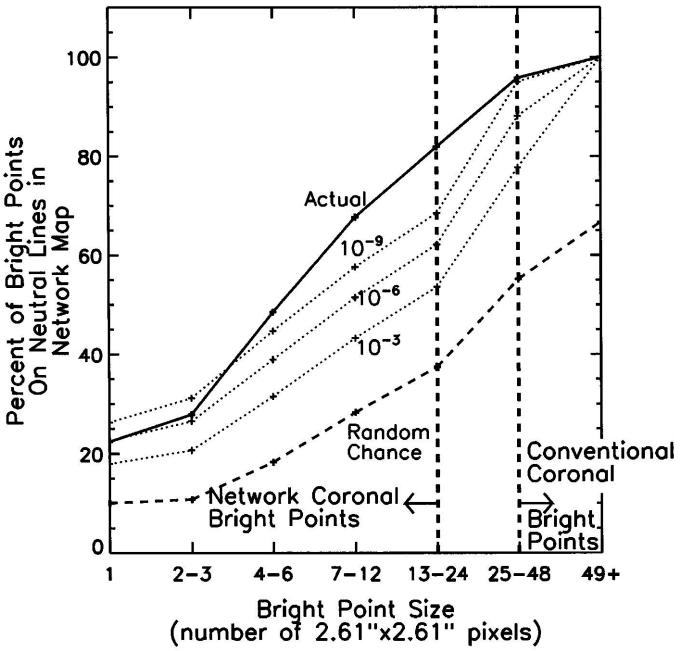


FIG. 9.—Quantification of the highly significant tendency of the small coronal bright points to sit on polarity dividing lines in the network magnetic flux. By the same method and symbols as in Fig. 8, this graph shows the fraction of bright points that overlie or touch both magnetic polarities and the significance of the offset of that fraction above random chance. This shows that many more small bright points overlie mixed polarity than would be expected by random chance. The fact that the coincidence with observed neutral lines falls off steeply with decreasing bright point size suggests that most of the seemingly unipolar small coronal bright points actually mark the presence of unresolved opposite polarity flux.

off in the coincidence of smaller bright points with network magnetic flux (Fig. 8) is much less than the drop off in their coincidence with neutral lines (Fig. 9) also suggests the presence of unresolved or transient fine-scale inclusions of opposite polarity flux in the network.

Why do some small bright points fail to overlie or touch magnetic areas of the magnetic network? The most obvious reason is that many of our small enhanced features might not be bright points but cosmic-ray strikes that would not be correlated with the network. We have many clear examples of cosmic-ray strikes in our sample, but we decided not to remove them since it quickly would become a judgement call and we might remove actual small bright points. Furthermore, their removal would just improve the already impressive statistics. From off the limb counts of cosmic-ray strikes, we estimate that cosmic-ray strikes made at least half of the smallest bright points (1–3 pixels) that were found in the network cell interiors. Some other small bright points that fail appear to be the result of two or more larger faint loops overlapping along the line of sight over a network cell interior. Finally, some of the smallest bright points not in or touching the magnetic network are over fine-scale magnetic flux that is suppressed inside the cells in the network maps.

## 4. SUMMARY AND DISCUSSION

By employing suitable image processing of Fe XII coronal images and concurrent low-noise, high-sensitivity magnetograms, we have found the following results bearing on the magnetic origins of coronal heating in quiet regions:

1. Enhanced coronal structures of sub-supergranular scale form a network that roughly coincides with the magnetic network defined by the photospheric magnetic flux. The enhanced coronal network covers somewhat less than half of the area in quiet regions, but most of it is only a few percent brighter than the cell interiors, so that the entire coronal network contributes only about 5% of the total quiet-region Fe XII coronal emission.

2. Small parts of the coronal network are enhanced by 30% or more above the local background and stand out as bright points. These network coronal bright points cover only about 2% of the area and contribute only 1%–2% of the Fe XII coronal emission from quiet regions.

3. About 90% of the coronal network bright points lie within or touch the magnetic flux area of the network. Most of the coronal network structure that extends well into or bridges over cell interiors is fainter than the bright points, but such structures often stem from near a bright point in the magnetic network.

4. About 45% of the network coronal bright points sit on neutral lines in the network magnetic flux. This correlation of network bright points with neutral lines has a probability of less than $10^{-11}$ of occurring by random chance. This suggests that the 55% of network bright points that appear to sit on magnetic flux of only one polarity actually mark the presence of included opposite polarity flux not resolved (or perhaps missed in time) by the magnetogram.

We infer from the above results that the network coronal bright points are seated in neutral-line core fields, and so are small counterparts to the bright coronal core features found on neutral lines in active regions. That is, we conclude that the network coronal bright points are markers of

active network core fields, just as coronal core features are markers of active core fields in active regions. From the observations of Falconer et al. (1997) of enhanced coronal heating in active regions, it appears that core-field activity often drives much more (as much as 10 times more) coronal heating in extended loops rooted around the core field than within the core field itself. This observation, and our finding of extensions of the coronal network stemming from the magnetic network lanes and often from near network bright points, suggests (1) that active network core fields may drive more heating in the extended corona, on field lines stemming from the network, than within the core fields, and (2) that many core fields may be actively driving significant extended coronal heating without showing themselves as network coronal bright points. In any case, as in active regions, if the network core fields are important drivers of the heating of the extended quiet corona, then they must be efficient engines in that they put out much more energy for remote coronal heating than is lost to local coronal heating.

In active regions, Falconer et al. (1997) found strongly sheared core fields to be more effective coronal heaters than weakly sheared ones. Whether the same holds true for network core fields is unknown and will probably remain so until vector magnetographs attain the sensitivity and spatial resolution to detect shear in network core fields. This will require a large solar telescope ($\geq 0.5$ m), and may well require the telescope to be placed above the atmosphere for sufficiently good seeing, as is planned for the Japan/US/UK/Solar-B Mission.

Falconer et al. (1997) also found that there is some additional factor or process besides the strength and shear of the core field that controls the level of activity or rate of driving of coronal heating within the core field and/or on extended loops stemming from around the core field. They proposed that this controlling process is magnetic flux cancellation at the photospheric neutral line within the core field. As in active regions, at any one time the core fields on many of the neutral lines in the network are apparently not active enough to show themselves in coronal images as network coronal bright points. Also as in active regions, it is plausible that the level of activity of a network core field might be set by the rate of flux cancellation at that neutral line. It is known that the network lanes are formed by the converging flows at the edges of the supergranules, and that new small-scale magnetic fields of mixed polarity continually emerge in the supergranular upflow and are swept into the network lanes (Wang et al. 1996). It is also known that in a large majority of the magnetic bipoles that produce conventional coronal bright points, the opposite polarity flux is converging and canceling rather than emerging and separating (Harvey 1985). Thus, it is entirely plausible that the network coronal bright points mark core fields undergoing episodes of flux cancellation. We plan to test this possibility by combining *SOHO*/EIT Fe XII images with magnetogram movies of the magnetic network from the Michelson Doppler Imager on *SOHO*.

We thank the *SOHO*/EIT experiment team for providing the coronal images, and we appreciate help from Joe Gurman in handling this data. We thank Ed Reichmann for help in collecting the data, and Bob Wilson for discussions of probability theory. The paper was substantially improved by suggestions from the referee, Harrison Jones. NSO/Kitt Peak data used here are produced cooperatively by NSF/NOAO, NASA/GSFC, and NOAA/SEL. This work is part of a SOHO Guest Investigation funded by the Solar Physics Branch of NASA's Office of Space Science. This work was performed while D. A. Falconer held a National Research Council-MSFC Research Associateship.

## REFERENCES

Delaboudiniere, J.-P., et al. 1995, Sol. Phys., 162, 291
Dowdy, J. F., Jr., Rabin, D., & Moore, R. L. 1986, Sol. Phys., 105, 35
Falconer, D. A., Moore, R. L., Porter, J. G., Gary, G. A., & Shimizu, T. 1997, ApJ, 482, 519
Habbal, S. R., & Withbroe, G. L. 1981, Sol. Phys., 69, 77
Harvey, K. L. 1985, Australian J. Phys., 38, 875
Jones, H. P., Duvall, T. L., Jr., Harvey, J. W., Mahaffey, C. T., Schwitters, J. D., & Simmons, J. E. 1992, Sol. Phys., 139, 211
Koutchmy, S. 1977, in Illustrated Glossary for Solar and Solar-Terrestrial Physics, ed. A. Bruzek & C. J. Durrant (Dordrecht: Reidel), 39
Martres, M. J., & Bruzek, A. 1977, in Illustrated Glossary for Solar and Solar-Terrestrial Physics, ed. A Bruzek & C. J. Durrant (Dordrecht: Reidel), 53
Nolte, J. T., Solodyna, C. V., & Gerassimenko, M. 1979, Sol. Phys., 63, 113
Porter, J. G., Moore, R. L., Reichmann, E. J., Engvold, O., & Harvey, K. L. 1987, ApJ, 323, 380
Vaiana, G. S., & Rosner, R. 1978, ARA&A, 16, 393
Wang, H., Tang, F., Zirin, H., & Wang, J. 1996, Sol. Phys., 165, 223
Wang, H., Zirin, H., & Ai, G. 1991, Sol. Phys., 131, 53